RSC Advances

PAPER

View Article Online
View Journal | View Issue

Cite this: *RSC Adv.*, 2020, **10**, 19397

A triflate and alkynyl protected Ag_{43} nanocluster with a passivated surface†

Ting Li,‡[a] Xiaoqin Cui,‡[b] Linfeng Liang,[b] Cui Luo,[b] Huan Li*[b] and Xian-Ming Zhang*[ab]

Received 9th February 2020
Accepted 13th May 2020

DOI: 10.1039/d0ra01244k

rsc.li/rsc-advances

A trifluoromethanesulfonate (OTf) and *tert*-butylacetylene (^{t}BuC≡C$^-$) co-protected silver nanocluster (NC), $Ag_{43}(^t BuC{\equiv}C)_{24}(CF_3SO_3)_8$ (Ag_{43}), was synthesized and characterized. Single crystal X-ray diffraction analysis revealed its total structure. 43 Ag atoms are arranged into a three-concentric-shell $Ag@Ag_{12}@Ag_{30}$ structure. Both OTf and ^{t}BuC≡C$^-$ ligands bonded with Ag atoms in a μ_3 mode. The application of Ag_{43} as a catalyst for the reaction of silane with alcohol or H_2O indicated that the surface ligands had a profound passivation effect, which significantly influenced the reactivity and selectivity.

Introduction

Metal NCs have attracted a great amount of attention during the past decades not only for their aesthetic values but also for their potential applications in self-assembly, surface plasmon resonance (SPR), bio-markers, (electro)catalysis, *etc.*[1–6] Fundamentally relating their structures with their properties, however, has encountered huge challenges.[7] One obstacle is the difficulty in precisely characterizing the structures of NCs. To this end, many practical methodologies have been brought forward. Among them, single-crystal crystallography has special advantages in determining the total structures of NCs.[8] Aiming to resolve the target's structure at atomic level, this methodology has found incomparable advantage in revealing the organic–metal interfacial structure of NCs. For example, the unprecedented "staple" bonding motif of thiolate of Au_{102} NC was firstly revealed by this method.[9,10] There has since been a boom in the study of the potential applications of the atomically precise NCs, especially catalysis.[11] The promoting effect of the surface ligands have been repeatedly observed in different types of reactions.[12,13] However, to obtain the single crystals of NCs, the strong interaction between the NCs and ligands is usually necessary for stabilizing the NCs. Thus, the surface catalytically active sites might be blocked by the organic ligands. However, the researches addressing this issue of Ag NCs seem rare.

On the other side, a large number of thiolate and(or) phosphine protected Au or Ag NCs have been synthesized so far, such as Au_{25},[14] Au_{38},[15] Au_{279},[16] Ag_{40},[17] Ag_{44},[18,19] Ag_{67},[20] Ag_{146},[21] Ag_{141},[22] and many others.[23] Beyond the conventional ligands, alkynes are drawing fast-increasing attentions, thanks to the flexible bonding modes of alkynes with metals.[24–28] In recent years, there have been a considerable amount of NCs containing anions in their structures. Most of them, however, function as templates or counterions.[29–32] Ag NCs or complexes featuring direct Ag–O bonding are mostly those with Ag(I) species.[33] Examples of Ag(0) NCs protected by inorganic oxo anions are rare. Sun *etc.* recently reported a Ag(0) NC co-protected by CrO_4^{2-} and ^{t}BuC≡C$^-$, $[Ag_{48}(C{\equiv}C^tBu)_{20}(CrO_4)_7]$.[34] Herein, we report the first example of a Ag(0) NC co-protected by triflate (OTf) and *tert*-butylacetylene (^{t}BuC≡C$^-$), namely, $Ag_{43}(^t BuC{\equiv}C)_{24}(CF_3SO_3)_8$ (denoted as Ag_{43}). The detailed structure of Ag_{43} is analyzed and discussed. Significantly, we have found a strong passivation effect in the reaction of silanes with alcohol or H_2O catalyzed by Ag_{43}. This effect not only sharply decreased the reaction rate, but also exerted a direct influence on the reaction selectivity.

Results and discussion

Ag_{43} was synthesized by introducing a reducing agent, $NaBH_4$ into an ethanol solution of $AgSO_3CF_3$, *tert*-butylacetylene (^{t}BuC≡C$^-$), 1,4-bis-(diphenylphosphino)butane (dppb), and triethylamine (Et_3N). The reaction was aged for 24 hours during which the colour gradually changed from pale-yellow to dark green. A block-shaped single crystal was obtained by slowly diffusing a mixed solvent of hexane and ether into the mother solution (ESI, Fig. S1†). Ag_{43} crystallizes in *I*2/*m* space group and its overall structure is shown in Fig. 1 and S2.† It consists of 43 silver atoms, 24 ^{t}BuC≡C$^-$ and 8 OTf ligands. The Ag atoms are arranged into a three-shell Russian doll structure, $Ag@Ag_{12}@Ag_{30}$ (Fig. 1b). The $Ag@Ag_{12}$ shells make up an icosahedron with a dodeca-coordinated Ag atom at the center (Fig. 1c). Bearing a Ag atom bonding with only Ag atoms endows Ag_{43} with partial

[a]*School of Chemistry & Material Science, Shanxi Normal University, Linfen, 041004, China. E-mail: xmzhang@sxu.edu.cn*

[b]*Institute of Crystalline Materials, Shanxi University, Taiyuan, 030006, China. E-mail: 59584340@sxu.edu.cn*

† Electronic supplementary information (ESI) available. CCDC 1981614. For ESI and crystallographic data in CIF or other electronic format see DOI: 10.1039/d0ra01244k

‡ These authors contributed equally to this work.

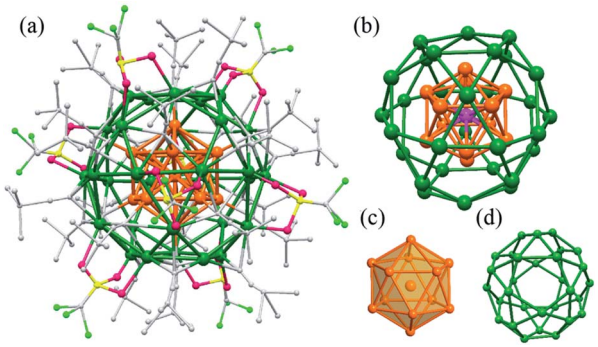

Fig. 1 (a) The overall structure of $Ag_{43}(^tBuC{\equiv}C)_{24}(CF_3SO_3)_8$, Ag_{43}. (b) The three shells of $Ag@Ag_{12}@Ag_{30}$. (c) The $Ag@Ag_{12}$ centered icosahedron. (d) The outer Ag_{30} shell. Color legend: olive green and orange, Ag; pink, O; yellow, S; light green, F; gray, C. H atoms are omitted for clarity.

Ag(0) character. The rest 30 Ag atoms of the outermost shell form 12 pentagons and 20 triangles. The two regular polygons are connected through edge-sharing, which makes each pentagon be enclosed by five triangles and each triangle by three pentagons. Geometrically, such an arrangement forms an icosidodecahedron, an Archimedean solid (Fig. 1d). The outermost shell is closely related with the ligands' distribution (see below). The average Ag–Ag bond length between the central Ag to Ag_{12} shell is 2.858 Å, while the value is 3.1 Å between Ag_{12} and Ag_{30} shells. Both are less than the sum of the van der Waals radii of two Ag atoms (3.44 Å), indicating argyrophilic interactions between the shells.

As mentioned, the distribution of peripheral ligands is dependent on the arrangement of silver atoms, especially the Ag_{30} shell (Fig. 2a). There are 24 $^tBuC{\equiv}C^-$ ligands which can be equally divided into two groups. Each of the first half penetrates one of the twelve pentagons of Ag_{30} shell and bonded to Ag_{12} shell through σ bond. Each of the twelve $^tBuC{\equiv}C^-$ also bonds

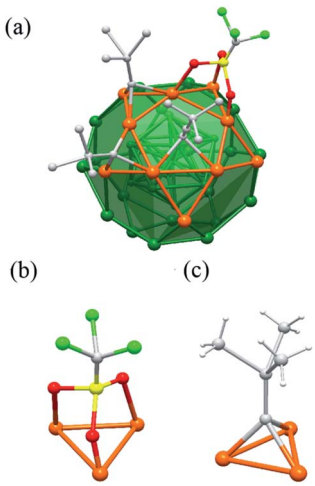

Fig. 2 (a) The coordination mode of Ag_{43} surface ligands. The μ_3 bonding motifs of OTf (b) and $^tBuC{\equiv}C^-$ (c) with the Ag_{30} shell. For clarity, only parts of the ligands are shown.

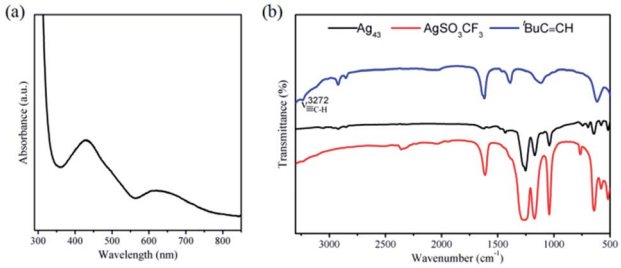

Fig. 3 (a) UV-vis absorption spectrum of Ag_{43} in CH_2Cl_2 solution. (b) FT-IR spectrum of Ag_{43} (black), $^tBuC{\equiv}C^-$ (blue) and $AgSO_3CF_3$ (red).

with the pentagon through π bonds (Fig. 2a). The rest 12 $^tBuC{\equiv}C^-$ ligands along with 8 OTf ligands, which amount to 20, coordinated with the 20 triangles of the Ag_{30} shell respectively. It is noteworthy that every $^tBuC{\equiv}C^-$ and OTf has the similar μ_3 coordination mode (Fig. 2b and c). It is also worth noting that although OTf bonding with Ag atoms are commonly seen in Ag(I) complexes or clusters, especially those with low nuclearity,[35,36] Ag(0) NC protected by OTf has barely been reported. The bond length of the Ag–O bond is 2.415 Å, which is within the common range typical Ag–O bonds.[37,38]

We investigated the optical properties of Ag_{43} in CH_2Cl_2 (Fig. 3). As illustrated in Fig. 3a, the UV-vis absorption spectrum of Ag_{43} shows two absorption features: one major peak at 434 nm and a shoulder at 620 nm. FT-IR spectra of Ag_{43}, $^tBuC{\equiv}C^-$ and the precursor $AgSO_3CF_3$ are shown in Fig. 3b. The stretching of ≡C–H at 3272 cm^{-1} is no longer present in Ag_{43}, indicating the bonding of $^tBuC{\equiv}C^-$ with Ag.[39] The characteristic peaks of $SO_3CF_3^-$ ranging from 1000 to 1500 cm^{-1}, on the other hand, are still prominent in the spectrum of Ag_{43}. These information further confirmed both ligands are present on Ag_{43}.

The possible influence of the Ag_{43} surface ligands on catalysis was evaluated in the reaction of a sterically demanding substrate dimethylphenylsilane (denoted as silane) with H_2O or 1-butanol (Scheme 1).[40,41] As a benchmark, polyvinylpyrrolidone (PVP) stabilized Ag nanoparticles (Ag/PVP) were also fabricated following a reported procedure.[42] The results are summarized in

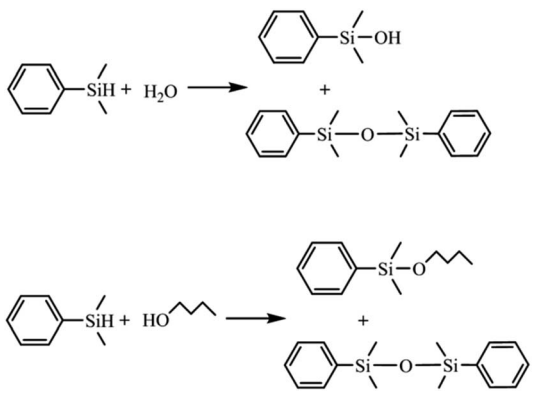

Scheme 1 Reaction scheme of silane with H_2O and 1-butanol. The side reaction is the condensation of two silane molecules.

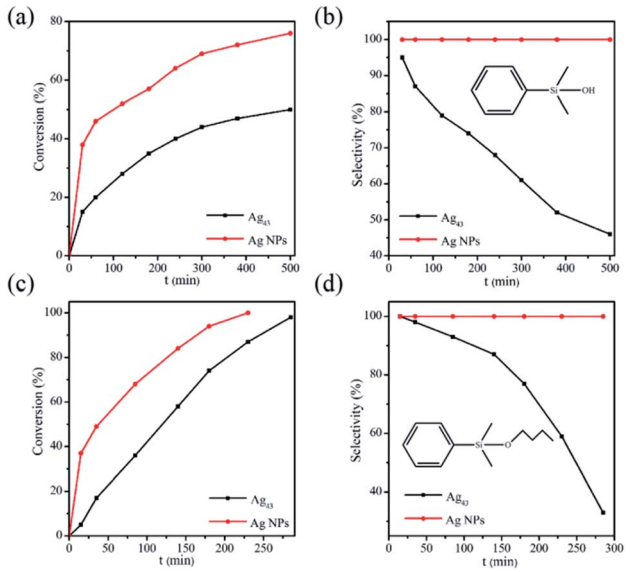

Fig. 4 Tracing the reaction of silane with H_2O catalyzed by Ag_{43} or Ag/PVP. (a) Conversion of silane and (b) the selectivity towards the target whose structure is shown in the figure. (c and d) are those for silane reacting with butanol. Reaction conditions: Ag (0.2 mmol), dimethylphenylsilane (2 mmol), H_2O or 1-butanol (22 mmol), toluene (2 mL), 30 °C. The byproduct is 1,3-diphenyl-1,1,3,3-tetramethyldisiloxane for both reactions.

Fig. 4. We can see that for either H_2O or alcohol as substrate, the reaction catalyzed by Ag_{43} always showed significantly lower reactivity than Ag/PVP, although the amount of Ag as well as the other reaction conditions were kept the same (Fig. 4a and c). Despite the small size of Ag_{43} (less than 1 nm), the surface ligands still exerted a direct impact on limiting the contact of substrate with Ag. This also influenced the product distribution. For Ag/PVP, full selectivity towards the target was always achieved. Ag_{43}, however, afforded a significant amount of 1,3-diphenyl-1,1,3,3-tetramethyldisiloxane (denoted as disiloxane). As the reaction proceeded, the byproduct kept accumulating. For example, in hydrolysis reaction catalyzed by Ag_{43}, when half the silane was consumed, the byproduct disiloxane accounted for 54% of the total product (Fig. 4b). The situation was similar in dehydrogenative coupling with 1-butanol (Fig. 4d). Not only the reaction rate was slower for Ag_{43}, but disiloxane was also found as a major part of the products. Ag was fairly stable under such reaction condition. The light absorption Ag_{43} after reaction has similar features (Fig. S3†). Generally, the rate-limiting step of this reaction is the activation of alcohol. Thus, given the full occupation of the surface Ag site, this step might be inhibited, which gave silane more chance to react with each other. The exact mechanism, however, still requires further thorough investigation.

Conclusions

In conclusion, a triflate and *tert*-butylacetylene protected Ag_{43} is synthesized and characterized. For the first time the triflate is shown to function as an effective surface ligand for Ag(0) nanocluster. It bonds with Ag atoms in μ_3 mode. Although Ag_{43} has a very small size, its catalytic ability is significantly worse than the PVP protected Ag nanoparticles. The surface ligands of Ag_{43} showed strong passivation effect for the reaction of silane with H_2O or butanol. Such an effect also sharply decreased the selectivity towards the desired target, yielding a significant percentage of disiloxane as byproduct.

Conflicts of interest

There are no conflicts to declare.

Acknowledgements

We express our gratitude to National Natural Science Foundation of China (21972080, 21503123, 91961201 & 21871167), Sanjin Scholar, Shanxi "1331 Project" Key Innovative Research Team for financial support. We are also grateful for the help from the State Key Laboratory for Physical Chemistry of Solid Surfaces of Xiamen University.

Notes and references

1 Z. Wu, Q. Yao, S. Zang and J. Xie, *ACS Mater. Lett.*, 2019, **1**, 237–248.
2 T. Higaki, Y. Li, S. Zhao, Q. Li, S. Li, X.-S. Du, S. Yang, J. Chai and R. Jin, *Angew. Chem. Int. Ed.*, 2019, **58**, 8291–8302.
3 J. Chai, H. Chong, S. Wang, S. Yang, M. Wu and M. Zhu, *RSC Adv.*, 2016, **6**, 111399–111405.
4 Y. Wang, J. Zhang, L. Huang, D. He, L. Ma, J. Ouyang and F. Jiang, *Chem.–Eur. J.*, 2012, **18**, 1432–1437.
5 H. Qian, D.-E. Jiang, G. Li, C. Gayathri, A. Das, R. R. Gil and R. Jin, *J. Am. Chem. Soc.*, 2012, **134**, 16159–16162.
6 C.-A. J. Lin, C.-H. Lee, J.-T. Hsieh, H.-H. Wang, J. K. Li, J.-L. Shen, W.-H. Chan, H.-I. Yeh and W. H. Chang, *J. Med. Biol. Eng.*, 2009, **29**, 276–283.
7 A. W. Cook and T. W. Hayton, *Acc. Chem. Res.*, 2018, **51**, 2456–2464.
8 L. J. Farrugia, *J. Appl. Crystallogr.*, 1999, **32**, 837–838.
9 D.-e. Jiang, M. L. Tiago, W. Luo and S. Dai, *J. Am. Chem. Soc.*, 2008, **130**, 2777–2779.
10 P. D. Jadzinsky, G. Calero, C. J. Ackerson, D. A. Bushnell and R. D. Kornberg, *Science*, 2007, **318**, 430–433.
11 G. Li and R. Jin, *Acc. Chem. Res.*, 2013, **46**, 1749–1758.
12 Y. Wang, X.-K. Wan, L. Ren, H. Su, G. Li, S. Malola, S. Lin, Z. Tang, H. Häkkinen, B. K. Teo, Q.-M. Wang and N. Zheng, *J. Am. Chem. Soc.*, 2016, **138**, 3278–3281.
13 X.-K. Wan, J.-Q. Wang, Z.-A. Nan and Q.-M. Wang, *Sci. Adv.*, 2017, **3**, e1701823.
14 Z. Wu, J. Suhan and R. Jin, *J. Mater. Chem.*, 2009, **19**, 622–626.
15 R. L. Donkers, D. Lee and R. W. Murray, *Langmuir*, 2004, **20**, 1945–1952.
16 N. A. Sakthivel, S. Theivendran, V. Ganeshraj, A. G. Oliver and A. Dass, *J. Am. Chem. Soc.*, 2017, **139**, 15450–15459.
17 J. Chai, S. Yang, Y. Lv, T. Chen, S. Wang, H. Yu and M. Zhu, *J. Am. Chem. Soc.*, 2018, **140**, 15582–15585.

18 H. Yang, Y. Wang, H. Huang, L. Gell, L. Lehtovaara, S. Malola, H. Häkkinen and N. Zheng, *Nat. Commun.*, 2013, **4**, 2422.
19 Y. Cao, J. Guo, R. Shi, G. I. N. Waterhouse, J. Pan, Z. Du, Q. Yao, L.-Z. Wu, C.-H. Tung, J. Xie and T. Zhang, *Nat. Commun.*, 2018, **9**, 2379–2384.
20 M. J. Alhilaly, M. S. Bootharaju, C. P. Joshi, T. M. Besong, A. H. Emwas, R. Juarez-Mosqueda, S. Kaappa, S. Malola, K. Adil, A. Shkurenko, H. Häkkinen, M. Eddaoudi and O. M. Bakr, *J. Am. Chem. Soc.*, 2016, **138**, 14727–14732.
21 Y. Song, K. Lambright, M. Zhou, K. Kirschbaum, J. Xiang, A. Xia, M. Zhu and R. Jin, *Nanoscale*, 2018, **12**, 9318–9325.
22 L. Ren, P. Yuan, H. Su, S. Malola, S. Lin, Z. Tang, B. K. Teo, H. Häkkinen, L. Zheng and N. Zheng, *J. Am. Chem. Soc.*, 2017, **139**, 13288–13291.
23 J. Yan, B. K. Teo and N. Zheng, *Acc. Chem. Res.*, 2018, **51**, 3084–3093.
24 Z. Lei, X.-K. Wan, S.-F. Yuan, Z.-J. Guan and Q.-M. Wang, *Acc. Chem. Res.*, 2018, **51**, 2465–2474.
25 X.-K. Wan, Z.-J. Guan and Q.-M. Wang, *Angew. Chem. Int. Ed.*, 2017, **56**, 11494–11497.
26 M. Qu, H. Li, L.-H. Xie, S.-T. Yan, J.-R. Li, J.-H. Wang, C.-Y. Wei, Y.-W. Wu and X.-M. Zhang, *J. Am. Chem. Soc.*, 2017, **139**, 12346–12349.
27 G.-X. Duan, L. Tian, J.-B. Wen, L.-Y. Li, Y.-P. Xie and X. Lu, *Nanoscale*, 2018, **10**, 18915–18919.
28 S.-F. Yuan, P. Li, Q. Tang, X.-K. Wan, Z.-A. Nan, D. Jiang and Q.-M. Wang, *Nanoscale*, 2017, **9**, 11405–11409.
29 Q. M. Wang, Y. M. Lin and K. G. Liu, *Acc. Chem. Res.*, 2015, **48**, 1570–1579.
30 S.-D. Bian, H.-B. Wu and Q.-M. Wang, *Angew. Chem. Int. Ed.*, 2009, **48**, 5363–5365.
31 Z. Wang, R. K. Gupta, G. G. Luo and D. Sun, *Chem. Rec.*, 2020, **20**, 389–402.
32 S.-D. Bian, J.-H. Jia and Q.-M. Wang, *J. Am. Chem. Soc.*, 2009, **131**, 3422–3423.
33 R. Terroba, M. B. Hursthouse, M. Laguna and A. Mendia, *Polyhedron*, 1999, **18**, 807–810.
34 S. S. Zhang, F. Alkan, H. F. Su, C. M. Aikens, C. H. Tung and D. Sun, *J. Am. Chem. Soc.*, 2019, **141**, 4460–4467.
35 S. L. James, D. M. P. Mingos, A. J. P. White and D. J. Williams, *Chem. Commun.*, 1998, 2323–2324.
36 M. Bardají, O. Crespo, A. Laguna and A. K. Fischer, *Inorg. Chim. Acta*, 2000, **304**, 7–16.
37 I. Diez and R. H. Ras, *Nanoscale*, 2011, **3**, 1963–1970.
38 Z. Wang, H. F. Su, C. H. Tung, D. Sun and L. S. Zheng, *Nat. Commun.*, 2018, **9**, 2094.
39 M. Qu, F.-Q. Zhang, D.-H. Wang, H. Li, J.-J. Hou and X.-M. Zhang, *Angew. Chem. Int. Ed.*, 2020, **132**, 6569–6574.
40 A. Dhakshinamoorthy, I. E. Adell, A. Primo and H. Garcia, *ACS Sustain. Chem. Eng.*, 2017, **5**, 2400–2462.
41 Y. Kikukawa, Y. Kuroda, K. Yamaguchi and N. Mizuno, *Angew. Chem. Int. Ed.*, 2012, **51**, 2434–2437.
42 H. Wang, X. Qiao, J. Chen and S. Ding, *Colloids Surf. A Physicochem. Eng. Asp.*, 2005, **256**, 111–115.